SRTTU

JCARME
ISSN: 2228-7922
Journal of Computational and Applied Research
in Mechanical Engineering
Vol. 8, No. 2, pp. 223-234
jcarme.sru.ac.ir

Three-dimensional characteristic approach for incompressible thermo-flows and influence of artificial compressibility parameter

A. Tohid Adibi*

Department of mechanical engineering, University of Bonab, 5551761167, Bonab, Iran

Article info:

Received: 11/11/2016
Accepted: 24/08/2018
Online: 26/08/2018

Keywords:
Three-dimensional characteristics,
Incompressible flow,
Artificial compressibility,
Convergence history,
Energy equation.

Abstract

In this paper, obtaining the characteristics of unsteady three-dimensional incompressible flows with heat transfer along with artificial compressibility of Chorin is investigated. At first, compatibility equations and pseudo characteristics for three-dimensional flows are derived from five governing equations (continuity equation, momentum equations in three directions, and energy equation) and then results are simplified to two-dimensional flows. Pseudo Mach hyper-cone (four-dimensional cone) is found, and its cross-section with physical axis is calculated numerically. Unlike compressible flow, this is not a sphere. It is found that the pseudo-acoustic speed within the incompressible flow is a function of the artificial compressibility parameter and the directions. In two-dimensional flow, Pseudo Mach cone is obtained by numerical solution of characteristic equations. Unlike compressible flow, the cross-section of Mach cone with the x-y plane is not a circle. This shape is not oval, too. The influence of artificial compressibility parameter on convergence history and accuracy is surveyed by simulation of cavity flow as a benchmark.

Nomenclature

1D	One-dimensional
2D	Two-dimensional
3D	Three-dimensional
AC	Artificial compressibility
CB	Characteristic based
FVM	Finite volume methodology
g	Gravitational acceleration
Gr	Grashof number
HACB	High-accuracy characteristics-based
k	Thermal conductivity
LBM	Lattice Boltzmann method
M	Number of cells in x-direction
Pr	Prandtl number
Re	Reynolds number
T	Temperature
t	Time
u, v, w	x, y, z velocity components
x, y, z	Coordinates
W	Vector on characteristic hyper surface

Greek symbols

β	Artificial compressibility coefficient
βex	Thermal expansion coefficient
σ	Arbitrary and constant number
μ	Coefficient of viscosity
MC	Multidimensional characteristic
MCB	Multidimensional characteristic-based
N	Number of cells in y-direction
Nu	Local Nusselt number
p	Pressure
υ	Kinematic viscosity
ρ	Density

Subscripts

ref	Reference

*Corresponding author
email address: tohidadibi@gmail.com

1. Introduction

Many numerical schemes for incompressible flows with heat transfer are mainly based on pressure corrections. AC is the other method. In this method, $\frac{1}{\beta}\frac{\partial p}{\partial t}$ is added to the continuity equation. So the continuity and the momentum equations are coupled, and then the governing equations become hyperbolic and accept the compressible flow schemes. For the first time, the characteristic methods are used for incompressible flows by Drikakis et al. [1]. Razavi and Adibi [2] proposed a new characteristic-based approach for thermo-flow with FVM in which MC scheme is applied for convective fluxes. AC is used, and as a result, the governing equations take the hyperbolic nature. To obtain compatibility equations and pseudo characteristics, the energy equation is taken into account in the MC scheme. They simulated forced convection between parallel plates, as well as forced and mixed convection in a cavity as a benchmark for a wide range of Reynolds, Grashof, and Prandtl numbers. Their results confirm the robustness of the MC scheme in terms of accuracy and convergence and are in good agreement with the standard benchmark solutions in the literature. In other work, Adibi and Razavi [3] used their scheme to simulate flow across circular cylinder. They showed that their scheme can be used for non-Cartesian grids. They used secondary cells to calculate viscous terms and fifth-order Rung-Kutta for time marching in their works. Razavi and Hanifi [4] developed a new characteristic method for turbulent flows. Zamzamian and Razavi [5], Fathollahi and Zamanian [6] and Abdollahi et al. [7] extended the characteristic-based method and used the obtained equations to simulate different incompressible flows.

Franklin and Harris [8] present a high-order upwind finite-difference scheme for solving a useful family of first-order partial differential equations. They showed that the proposed scheme is accurate and stable. Van der Velden et al. [9] improved a three-dimensional flow and developed an aero-acoustic solver in a finite-volume. As dispersion errors are usual in this scheme, Riemann fluxes are used to solve the linearized unsteady Euler equations. Kaviani and Nikkhah Bahrami [10] extended the 3D Navier–Stokes characteristic boundary conditions for large-eddy and aeroacoustic simulations to curvilinear coordinates formulations. They applied their new scheme to simulate four benchmarks.

Munir [11] established a numerical scheme based on AC formulation of a phase-field model for simulating two-phase incompressible flows. The coupled nonlinear systems composed of the incompressible Navier–Stokes equations; a volume preserving Allen–Cahn-type phase-field equation is reorganized into conservative form with source terms, which are suitable to implement high-resolution methods. Adibi et al. [12] simulated natural convection inside square and trapezoidal cavities numerically. In all simulations, the results presented in a variety of forms such as streamlines, isothermal lines, and velocity profiles. Moyne and Souto [13] calculated the average temperature fields with one and two-equation models and compared the results with an exact analytical solution in the particular case of a stratified medium.

Here, the characteristic methods are developed for 3D incompressible flow with heat transfer, and also mathematical structures of characteristics for incompressible thermo-flow in conjunction with AC are derived. By the aid of derived compatibility relations, a scheme for 3D incompressible flow with heat transfer is presented. So 2D relations are obtained from 3D relations and in the final part of this work, the influence of artificial incompressibility parameter on convergence history and accuracy is surveyed.

2. Three-dimensional characteristic based method

The governing equations for 3D incompressible thermo-flow can be expressed as:

$$\frac{\partial u}{\partial x}+\frac{\partial v}{\partial y}+\frac{\partial w}{\partial z}=0$$

$$\frac{\partial u}{\partial t}+u\frac{\partial u}{\partial x}+v\frac{\partial u}{\partial y}+w\frac{\partial u}{\partial z}=$$
$$-\frac{1}{\rho}\frac{\partial p}{\partial x}+\upsilon(\frac{\partial^2 u}{\partial x^2}+\frac{\partial^2 u}{\partial y^2}+\frac{\partial^2 u}{\partial z^2}),$$

$$\frac{\partial v}{\partial t}+u\frac{\partial v}{\partial x}+v\frac{\partial v}{\partial y}+w\frac{\partial v}{\partial z}=$$
$$-g-\frac{1}{\rho}\frac{\partial p}{\partial y}+\upsilon(\frac{\partial^2 v}{\partial x^2}+\frac{\partial^2 v}{\partial y^2}+\frac{\partial^2 v}{\partial z^2}),\qquad(1)$$

$$\frac{\partial w}{\partial t}+u\frac{\partial w}{\partial x}+v\frac{\partial w}{\partial y}+w\frac{\partial w}{\partial z}=$$
$$-\frac{1}{\rho}\frac{\partial p}{\partial y}+\upsilon(\frac{\partial^2 w}{\partial x^2}+\frac{\partial^2 w}{\partial y^2}+\frac{\partial^2 w}{\partial z^2}),$$

$$\frac{\partial T}{\partial t}+u\frac{\partial T}{\partial x}+v\frac{\partial T}{\partial y}+w\frac{\partial T}{\partial z}=$$
$$\frac{k}{\rho C_p}(\frac{\partial^2 T}{\partial x^2}+\frac{\partial^2 T}{\partial y^2}+\frac{\partial^2 T}{\partial z^2}).$$

In free and mixed convection, density is not constant, but the Boussinesq assumption can be used, so the y-momentum transforms to:

$$\frac{\partial v}{\partial t}+u\frac{\partial v}{\partial x}+v\frac{\partial v}{\partial y}+w\frac{\partial v}{\partial z}=$$
$$-g\beta_{ex}\rho(\mathrm{T}-\mathrm{T}_{ref})-\frac{1}{\rho}\frac{\partial p}{\partial y}+\qquad(2)$$
$$\upsilon(\frac{\partial^2 v}{\partial x^2}+\frac{\partial^2 v}{\partial y^2}+\frac{\partial^2 v}{\partial z^2}),$$

Artificial compressibility factor is added to the continuity equation. So this equation is changed to:

$$\frac{1}{\beta}\frac{\partial p}{\partial t}+\frac{\partial u}{\partial x}+\frac{\partial v}{\partial y}+\frac{\partial w}{\partial z}=0\qquad(3)$$

Eq. (3) can be transformed into dimensionless forms by:

$$u^*=\frac{u}{U_{ref}},\quad v^*=\frac{v}{U_{ref}},\quad w^*=\frac{w}{U_{ref}},$$
$$x^*=\frac{x}{L_{ref}},\quad y^*=\frac{y}{L_{ref}},\quad z^*=\frac{z}{L_{ref}},$$
$$p^*=\frac{p+\rho gy-p_\infty}{\rho_{ref}U_{ref}^2},\quad t^*=\frac{tU_{ref}}{L_{ref}},\qquad(4)$$
$$T^*=\frac{T-T_{ref\,1}}{T_{ref\,2}-T_{ref\,1}}.$$

The governing equations in dimensionless forms are displayed as follows:

$$\frac{1}{\beta}\frac{\partial p}{\partial t}+\frac{\partial u}{\partial x}+\frac{\partial v}{\partial y}+\frac{\partial w}{\partial z}=0$$

$$\frac{\partial u}{\partial t}+u\frac{\partial u}{\partial x}+v\frac{\partial u}{\partial y}+w\frac{\partial u}{\partial z}=$$
$$-\frac{\partial p}{\partial x}+\frac{1}{\mathrm{Re}}(\frac{\partial^2 u}{\partial x^2}+\frac{\partial^2 u}{\partial y^2}+\frac{\partial^2 u}{\partial z^2}),$$

$$\frac{\partial v}{\partial t}+u\frac{\partial v}{\partial x}+v\frac{\partial v}{\partial y}+w\frac{\partial v}{\partial z}=$$
$$-\frac{Gr}{\mathrm{Re}^2}T-\frac{\partial p}{\partial y}+\frac{1}{\mathrm{Re}}(\frac{\partial^2 v}{\partial x^2}+\frac{\partial^2 v}{\partial y^2}+\frac{\partial^2 v}{\partial z^2}),\qquad(5)$$

$$\frac{\partial w}{\partial t}+u\frac{\partial w}{\partial x}+v\frac{\partial w}{\partial y}+w\frac{\partial w}{\partial z}=$$
$$-\frac{\partial p}{\partial z}+\frac{1}{\mathrm{Re}}(\frac{\partial^2 w}{\partial x^2}+\frac{\partial^2 w}{\partial y^2}+\frac{\partial^2 w}{\partial z^2}),$$

$$\frac{\partial T}{\partial t}+u\frac{\partial T}{\partial x}+v\frac{\partial T}{\partial y}+w\frac{\partial T}{\partial z}=$$
$$\frac{1}{\mathrm{Re}\,\mathrm{Pr}}(\frac{\partial^2 T}{\partial x^2}+\frac{\partial^2 T}{\partial y^2}+\frac{\partial^2 T}{\partial z^2}).$$

These references depend on the numerical problem. In the above equations, stars are omitted and Reynolds, Prandtl, Grashof numbers are defined as:

$$\mathrm{Re}=\frac{\rho_{ref}u_{ref}L_{ref}}{\mu},\quad \mathrm{Pr}=\frac{c_p\mu}{k},$$
$$Gr=\frac{\beta_{ex}\,g\,(T_{ref\,2}-T_{ref\,1})L_{ref}^3}{\upsilon^2}.\qquad(6)$$

To determine the characteristics and compatibility equations, governing equations (the first derivatives) are multiplied by the unknown parameters, σ_1 to σ_5, and summed. Thus, one has:

$$\begin{aligned}
&\sigma_1 * Con. + \sigma_2 * x_{Mom.} + \sigma_3 * y_{Mom.} \\
&\quad + \sigma_4 * z_{Mom.} + \sigma_5 * enrg. = 0 \quad \rightarrow \\
&\sigma_1\left(\frac{\partial p}{\partial t} + \beta\frac{\partial u}{\partial x} + \beta\frac{\partial v}{\partial y} + \beta\frac{\partial w}{\partial z}\right) + \\
&\sigma_2\left(\frac{\partial u}{\partial t} + u\frac{\partial u}{\partial x} + v\frac{\partial u}{\partial y} + w\frac{\partial u}{\partial z} + \frac{\partial p}{\partial x}\right) \\
&+\sigma_3\left(\frac{\partial v}{\partial t} + u\frac{\partial v}{\partial x} + v\frac{\partial v}{\partial y} + w\frac{\partial v}{\partial z} + \frac{\partial p}{\partial y}\right) \\
&+\sigma_4\left(\frac{\partial w}{\partial t} + u\frac{\partial w}{\partial x} + v\frac{\partial w}{\partial y} + w\frac{\partial w}{\partial z} + \frac{\partial p}{\partial z}\right) \\
&+\sigma_5\left(\frac{\partial T}{\partial t} + u\frac{\partial T}{\partial x} + v\frac{\partial T}{\partial y} + w\frac{\partial T}{\partial z}\right) = 0.
\end{aligned} \tag{7}$$

The vectors with components which are the coefficients of the partial derivatives in Eq. (7) are defined as follows:

$$\begin{aligned}
&\mathbf{W}_1 = \sigma_2\mathbf{e_x} + \sigma_3\mathbf{e_y} + \sigma_4\mathbf{e_z} + \sigma_1\mathbf{e_t}, \\
&\mathbf{W}_2 = \left(\sigma_1\beta + u\sigma_2\right)\mathbf{e_x} + \\
&\quad v\sigma_2\mathbf{e_y} + w\sigma_2\mathbf{e_z} + \sigma_2\mathbf{e_t}, \\
&\mathbf{W}_3 = u\sigma_3\mathbf{e_x} + \left(\sigma_1\beta + v\sigma_3\right)\mathbf{e_y} \\
&\quad + w\sigma_3\mathbf{e_z} + \sigma_3\mathbf{e_t}, \\
&\mathbf{W}_4 = u\sigma_3\mathbf{e_x} + v\sigma_3\mathbf{e_y} + \\
&\quad \left(\sigma_1\beta + w\sigma_3\right)\mathbf{e_z} + \sigma_3\mathbf{e_t} \\
&\mathbf{W}_5 = u\sigma_5\mathbf{e_x} + v\sigma_5\mathbf{e_y} + \\
&\quad w\sigma_5\mathbf{e_z} + \sigma_5\mathbf{e_t}.
\end{aligned} \tag{8}$$

Now, the normal vectors of characteristic hyper-surfaces are defined as:

$$\begin{aligned}
&\mathbf{N}.\mathbf{W}_j = 0, \qquad j = 1, 2, 3, 4, 5, \\
&\mathbf{N} = n_x\mathbf{e_x} + n_y\mathbf{e_y} + n_z\mathbf{e_z} + n_t\mathbf{e_t},
\end{aligned} \tag{9}$$

Eq. (9) displays five equations with five unknowns. To have a nontrivial solution, the determinant of the coefficient matrix must be zero.

$$\begin{vmatrix}
n_t & n_x & n_y & n_z & 0 \\
\beta n_x & \Theta & 0 & 0 & 0 \\
\beta n_y & 0 & \Theta & 0 & 0 \\
0 & 0 & 0 & \Theta & 0 \\
0 & 0 & 0 & 0 & \Theta
\end{vmatrix} = 0, \tag{10}$$

$$\Theta = un_x + vn_y + + wn_z + n_t$$

It should be noted that Eq. (10) has five real roots which are displayed as:

(triple roots),

$$n_t = \frac{1}{2}\left(-un_x - vn_y - wn_z \pm \sqrt{(un_x + vn_y + wn_z)^2 + 4\beta}\right) = \xi \tag{11}$$

The tangent vector to characteristics is expressed as $\mathbf{L} = dx\ \mathbf{e_x} + dy\ \mathbf{e_y} + dz\ \mathbf{e_z} + dt\ \mathbf{e_t}$ which is perpendicular to normal vector (**N**). So characteristics are obtained by solving $\mathbf{N}.\mathbf{L} = 0$ and are displayed in Eqs. (12 and 13).

$$\frac{dx}{dt} = u, \quad \frac{dy}{dt} = v, \quad \frac{dz}{dt} = w \tag{12}$$

(three times)

$$\begin{aligned}
&\frac{dx}{dt} = -n_x\xi, \quad \frac{dy}{dt} = -n_y\xi, \\
&\frac{dz}{dt} = -n_z\xi.
\end{aligned} \tag{13}$$

The first equation display pseudo path line and the second one shows the characteristic hyper-surfaces. The cross-section of these hyper-surfaces by physical space is obtained with a numerical solution of Eq. (13) by choosing $n_x = \cos(\theta)\cos(\phi), \quad n_y = \sin(\theta)\cos(\phi), \quad n_z = \sin(\phi),$ and is shown in Fig. 1. This shape is a sphere incompressible flow because the sound speed is equal in all directions. But in incompressible flow with artificial compressibility, the sound speed depends on artificial compressibility parameter (β) and direction (n_x, n_y, n_z). So the shape in Fig. 1 is not a sphere. The first "n_t" is substituted by its value in Eq. (4) then:

$$\sigma_1 = 0, \qquad \sigma_2 = -\frac{n_y}{n_x}\sigma_3 - \frac{n_z}{n_x}\sigma_4, \tag{14}$$

$$\sigma_3,\ \sigma_4, \sigma_5 = arbitrary.$$

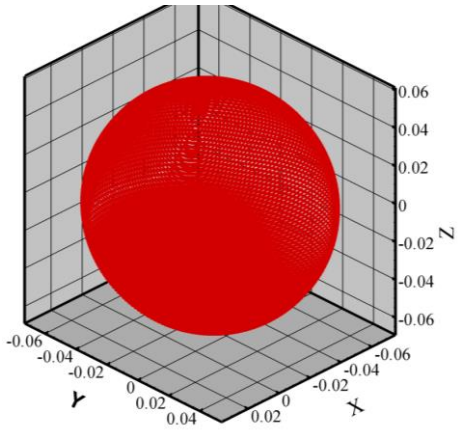

Fig. 1. Projection of four-dimensional space onto the three-dimensional physical space.

By choosing $\sigma_3 = 0,\ \sigma_4 = 0,\ \sigma_5 = 1$, the first compatibility equation is obtained as:

$$\frac{\partial T}{\partial t} + u\frac{\partial T}{\partial x} + v\frac{\partial T}{\partial y} + w\frac{\partial T}{\partial z} = 0 \rightarrow \frac{dT}{dt} = 0. \tag{15}$$

After discretization of the above equation on the characteristic line, one has:

$$\frac{dT}{dt} = 0 \rightarrow \frac{\Delta T}{\Delta t} = 0 \rightarrow \frac{T_*^{k+1} - T_c^{k}}{\Delta t} = 0 \rightarrow T_*^{k+1} = T_c^{k} \tag{16}$$

where "K" is the last level and "k+1" is the new level. "*" is the convective fluxes in the boundary of cells. Point "c" and point "*" are in the same characteristic line (Fig. 2). So the coordinates of point "c" is obtained by:

$$x_c = x_* - u\Delta t,\ y_c = y_* - v\Delta t,\ z_c = z_* - w\Delta t. \tag{17}$$

Then T_*^{k+1} is calculated by Eqs. (16 and 17). In this part, the velocities and the pressure should be calculated. So one needs:

$$(p^*)^{k+1},\ (u^*)^{k+1},\ (v^*)^{k+1} \text{and } (w^*)^{k+1}.$$

By choosing $\sigma_3 = 1,\ \sigma_4 = 0,\ \sigma_5 = 0$, and $\sigma_3 = 0,\ \sigma_4 = 1,\ \sigma_5 = 0$, the second and third compatibility equations are obtained as:

$$\begin{aligned} &\frac{-n_y}{n_x}\frac{\partial p}{\partial x} + \frac{\partial p}{\partial y} + \frac{-n_y}{n_x}\frac{du}{dt} + \frac{dv}{dt} = 0, \\ &\frac{-n_z}{n_x}\frac{\partial p}{\partial x} + \frac{\partial p}{\partial y} + \frac{-n_z}{n_x}\frac{du}{dt} + \frac{dw}{dt} = 0 \end{aligned} \tag{18}$$

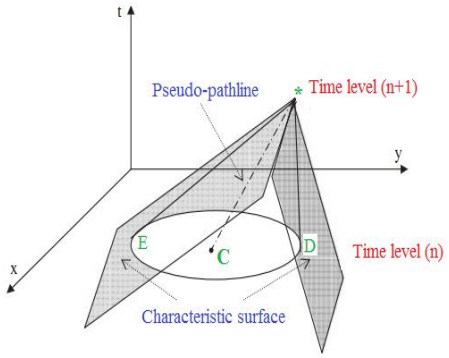

Fig. 2. Characteristic surfaces and pseudo path line [3].

Other compatibility equations are obtained in a similar way with other values of "n_t".

$$\sigma_1 = arbitrary,\quad \sigma_5 = 0,\ \sigma_2 = -n_x\xi\sigma_1,\quad \sigma_3 = -n_y\xi\sigma_1,\quad \sigma_4 = -n_z\xi\sigma_1$$

$$\begin{aligned} &\frac{\partial p}{\partial t} - n_x\xi\frac{\partial p}{\partial x} - n_y\xi\frac{\partial p}{\partial y} - n_z\xi\frac{\partial p}{\partial z} - \\ &n_x\xi\frac{\partial u}{\partial t} + (\beta - n_x\xi u)\frac{\partial u}{\partial x} - n_x\xi v\frac{\partial u}{\partial y} \\ &-n_x\xi w\frac{\partial u}{\partial z} - n_y\xi\frac{\partial v}{\partial t} - bu\frac{\partial v}{\partial x} \\ &+(\beta - n_y\xi v)\frac{\partial v}{\partial y} - n_y\xi w\frac{\partial v}{\partial z} \\ &-n_z\xi\frac{\partial w}{\partial t} - n_z\xi u\frac{\partial w}{\partial x} - n_z\xi v\frac{\partial w}{\partial y} \\ &+(\beta - n_z\xi w)\frac{\partial w}{\partial z} = 0 \end{aligned} \tag{19}$$

Unlike the first compatibility equation, the others do not recast into ODE. Therefore, one has to use 1D assumption to obtain the other compatibility equations. For this purpose, the previous procedure is carried out by considering 1D flow. Results are obtained as:

$$\frac{dp}{dt}-\frac{1}{2}(-u_n \pm u_a)\frac{du_n}{dt}=0,$$
$$u_a=\sqrt{u_n^2+\beta}$$
(compatibility equations) (20)
$$\frac{dx}{dt}=-\frac{1}{2}(-u_n \pm u_a)$$
(characteristic lines)

where u_n is the normal component of velocity (Fig. 3). After discretization and some mathematical calculations, velocity, pressure, and temperature are obtained by:

$$(u^*)^{k+1}=\frac{1}{u_a}((p_E)^k-(p_D)^k+\frac{1}{2}(u_n+u_a)(u_E)^k-\frac{1}{2}(u_n-u_a)(u_D)^k),$$
$$(p^*)^{k+1}=(p_E)^k-\frac{1}{2}(u_n+u_a)((u^*)^{k+1}-(u_E)^k),\quad (T^*)^{k+1}=(T_C)^k. \tag{21}$$

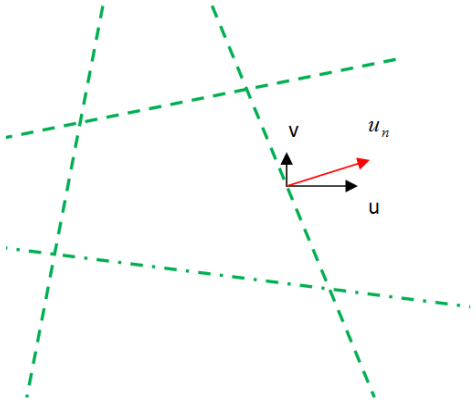

Fig. 3. The normal component of velocity in two-dimensional flows.

where u_n is the normal component of velocity (Fig. 2). After discretization of characteristic lines equation one has:

$$\frac{\Delta x}{\Delta t}=-\frac{1}{2}(-u_n \pm u_a)\rightarrow$$
$$\frac{x_*-x_E}{\Delta t}=-\frac{1}{2}(-u_n+u_a),$$
$$\frac{x_*-x_D}{\Delta t}=-\frac{1}{2}(-u_n-u_a), \tag{22}$$

where points "D" and "E" are on the characteristic lines (Fig. 2) and are obtained by the above equations. After discretization of compatibility equation one has:

$$\frac{\Delta p}{\Delta t}-\frac{1}{2}(-u_n \pm u_a)\frac{\Delta u_n}{\Delta t}=0\rightarrow$$
$$\frac{(p^*)^{k+1}-(p_E)^k}{\Delta t}-\frac{1}{2}(u_n+u_a)(\frac{(u^*)^{k+1}-(u_E)^k}{\Delta t})=0,$$
$$\frac{(p^*)^{k+1}-(p_D)^k}{\Delta t}-\frac{1}{2}(u_n-u_a)(\frac{(u^*)^{k+1}-(u_D)^k}{\Delta t})=0. \tag{23}$$
$$(u^*)^{k+1}=\frac{1}{u_a}((p_E)^k-(p_D)^k+\frac{1}{2}(u_n+u_a)(u_E)^k-\frac{1}{2}(u_n-u_a)(u_D)^k),$$
$$\frac{\Delta x}{\Delta t}=-\frac{1}{2}(-u_n \pm u_a)$$

where "k" is the last level and "k+1" is the new level. The point "*" is the convective fluxes in the boundary of cells. The $(p^*)^{k+1}$ and the $(u^*)^{k+1}$ are obtained by solving Eq. (23) simultaneously. Then:

$$(u^*)^{k+1}=\frac{1}{u_a}((p_E)^k-(p_D)^k+\frac{1}{2}(u_n+u_a)(u_E)^k-\frac{1}{2}(u_n-u_a)(u_D)^k),$$
$$(p^*)^{k+1}=(p_E)^k-\frac{1}{2}(u_n+u_a)((u^*)^{k+1}-(u_E)^k), \tag{24}$$

In this characteristic based method, the convective fluxes are calculated from the characteristic based method as is mentioned. The final results of this technique is:

$$
\begin{aligned}
&(\mathrm{u}^{*})^{k+1} = \frac{1}{u_a}((p_E)^k - (p_D)^k + \\
&\frac{1}{2}(u_n + u_a)(\mathrm{u}_E)^k - \frac{1}{2}(u_n - u_a)(\mathrm{u}_D)^k), \\
&(v^{*})^{k+1} = \frac{1}{2}(v^{k}_{i,j,m} + v^{k}_{i,j+1,m}), \\
&(Averaging\ \ method) \\
&(w^{*})^{k+1} = \frac{1}{2}(w^{k}_{i,j,m} + w^{k}_{i,j,m+1}), \\
&(Averaging\ \ method) \\
&(p^{*})^{k+1} = (p_E)^k - \frac{1}{2}(u_n + u_a) \\
&((\mathrm{u}^{*})^{k+1} - (\mathrm{u}_E)^k), \\
&T_{*}^{k+1} = T_c^{k}
\end{aligned}
\tag{25}
$$

In this section, the new characteristic method for 3D incompressible flow with heat transfer has been explained. In the next section, obtained equations are simplified to 2D incompressible flow with heat transfer.

3. Two-dimensional characteristic based method

In this part, the characteristic lines and the compatibility equations in 2D flows are obtained by eliminating z-direction. So the characteristic lines in 2D incompressible flow with heat transfer, are obtained by simplification of equations in the 3D flow. Consequently, Eqs. (25 and 26) are obtained from Eqs. (12 and 13). Then the characteristic line is:

$$
\frac{dx}{dt} = u, \quad \frac{dy}{dt} = v \ \text{(two times)} \tag{26}
$$

$$
\begin{aligned}
&\frac{dx}{dt} = \frac{-n_x}{2} \\
&\left(-un_x - vn_y \pm \sqrt{(un_x + vn_y)^2 + 4\beta}\right), \\
&\frac{dy}{dt} = \frac{-n_y}{2} \\
&\left(-un_x - vn_y \pm \sqrt{(un_x + vn_y)^2 + 4\beta}\right).
\end{aligned}
\tag{27}
$$

The Eq. (26) shows pseudo-pathline, and the Eq. (27) demonstrates the characteristic surfaces. These are shown in Fig. 2. By numerical solution of the above equations, the virtual Mach cone is obtained (Fig. 4). Similar to 3D state, in this part, another code is written in "MATLAB" software to obtain the numerical solution. Fig. 4 is the result of this code. For the numerical solution of the above equations, this procedure is done. The results of discretization of Eq. (26) are:

$$
\begin{aligned}
&x_{new} = x_0 + u(t_{new} - t_0), \\
&y_{new} = y_0 + v(t_{new} - t_0).
\end{aligned}
\tag{28}
$$

Discretization of Eq. (27) results in:

$$
\begin{aligned}
&x_{new} = x_0 + \frac{-n_x}{2}(-un_x - vn_y \pm \\
&\sqrt{(un_x + vn_y)^2 + 4\beta})(t_{new} - t_0), \\
&y_{new} = y_0 + \frac{-n_y}{2}(-un_x - vn_y \\
&\pm\sqrt{(un_x + vn_y)^2 + 4\beta})(t_{new} - t_0).
\end{aligned}
\tag{29}
$$

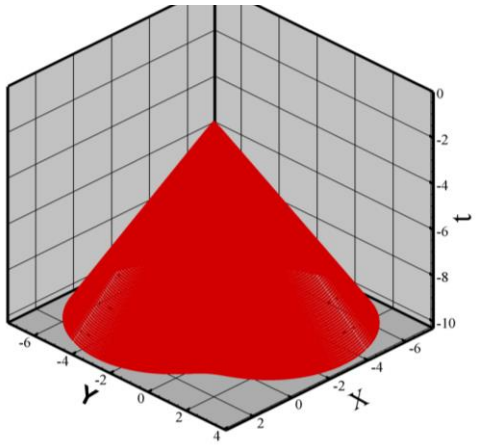

Fig. 4. Pseudo Mach cone for two-dimensional incompressible flow with artificial compressibility.

To obtain x_{new} , y_{new} , the n_x , n_y are defined as:

$$n_x = \cos(\theta) = \frac{x}{\sqrt{x^2 + y^2}}, \quad n_y = \sin(\theta) = \frac{y}{\sqrt{x^2 + y^2}}. \tag{30}$$

After the above procedure, for every new time, new "x" and "y" are obtained. So a new point with defined "x", "y" and "t" in the three-dimensional coordinate (x-y-t) can be defined. Fig. 4 is the shape contains mentioned the new point.

The cross-section of characteristic surfaces with the physical plane is obtained by defining $n_x = \cos(\theta)$, $n_y = \sin(\theta)$ and is displayed in Fig. 5 for different values of "β". Fig. 5 is the result of other code that is written in this research. In the compressible flow, this cross-section is a circle, but here it is not a circle or oval because the pseudo sound speed depends on the direction and is not constant. As $\sqrt{\beta}$ tends to larger values, the cross-section could become a circle. So, when $\sqrt{\beta} \to \infty$ Eq. (29) changes to:

$$x_{new} = x_0 + \sqrt{\beta}\cos(\theta)(t_{new} - t_0), \quad y_{new} = y_0 + \sqrt{\beta}\sin(\theta)(t_{new} - t_0). \tag{31}$$

In this case, $\sqrt{\beta}$ is the pseudo speed of sound in the incompressible flow. For compressible flow, one has:

$$x_{new} = x_0 + u(t_{new} - t_0),\ y_{new} = y_0 + v(t_{new} - t_0). \tag{32}$$

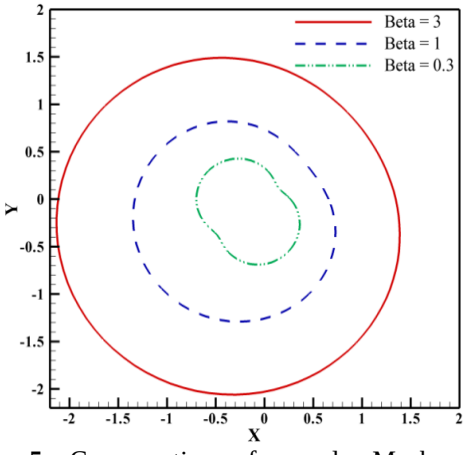

Fig. 5. Cross-section of pseudo Mach cone reforming in physical plane [2].

Comparison of Eqs. (31 and 32) shows that:

$$\sqrt{\beta} = \sqrt{u^2 + v^2} \to (compresible\ flow) \downarrow (incompressible\ flow) \tag{33}$$

In 2D flows, characteristic points "C, D, E" are obtained by Eq. (34) which are displayed in Figs. 6 and 7.

$$x_D = x^* - \frac{1}{2}(u_n - u_a)\Delta t, \quad x_E = x^* - \frac{1}{2}(u_n + u_a)\Delta t, \quad x_C = x^* - u\Delta t\ , \quad y_C = y^* - v\Delta t. \tag{34}$$

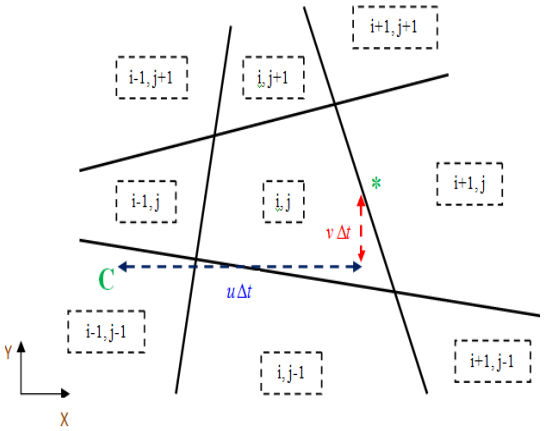

Fig. 6. Pattern for finding first characteristic point [3].

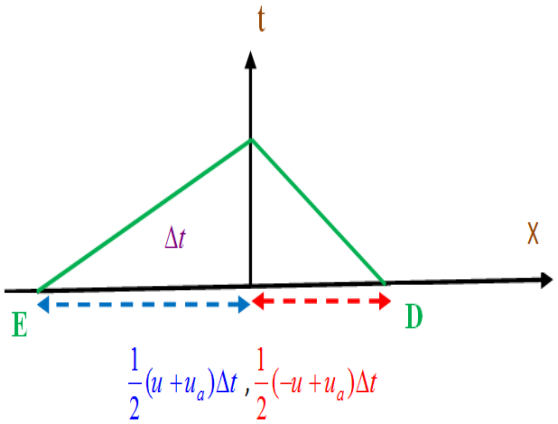

Fig. 7. Pattern for finding second and third characteristic point.

4. Influence of artificial compressibility parameter (β)

In this section, the influence of "β" is surveyed. The influence of "β" on the shape of the cone cross-section has been surveyed in the previous section and shown in Fig. 5. To investigate the influence of "β" on convergence history and accuracy, forced and natural convection in a cavity is simulated by new scheme with different "β" in different boundary conditions. For this purpose, a new code is written in FORTRAN software. Secondary cells are used for viscous terms, and fifth-order Rung-Kutta is used for time discretization as the authors' previous papers [2, 3]. The streamlines obtained by different "β" are shown and compared with that of Cheng and Liu [14] in Fig. 8. There is no significant difference between the results. Up and down wall Nusselt Numbers are shown and compared with those of Iwatsu et al. [15] in Figs. 9 and 10. Like recent results, there is not an important difference between the results. Error in each time-step is calculated by:

$$Error = \sqrt{\frac{\sum\sum\left(T_{i,j}^{n+1} - T_{i,j}^{n}\right)^2}{N * M}} \qquad (35)$$

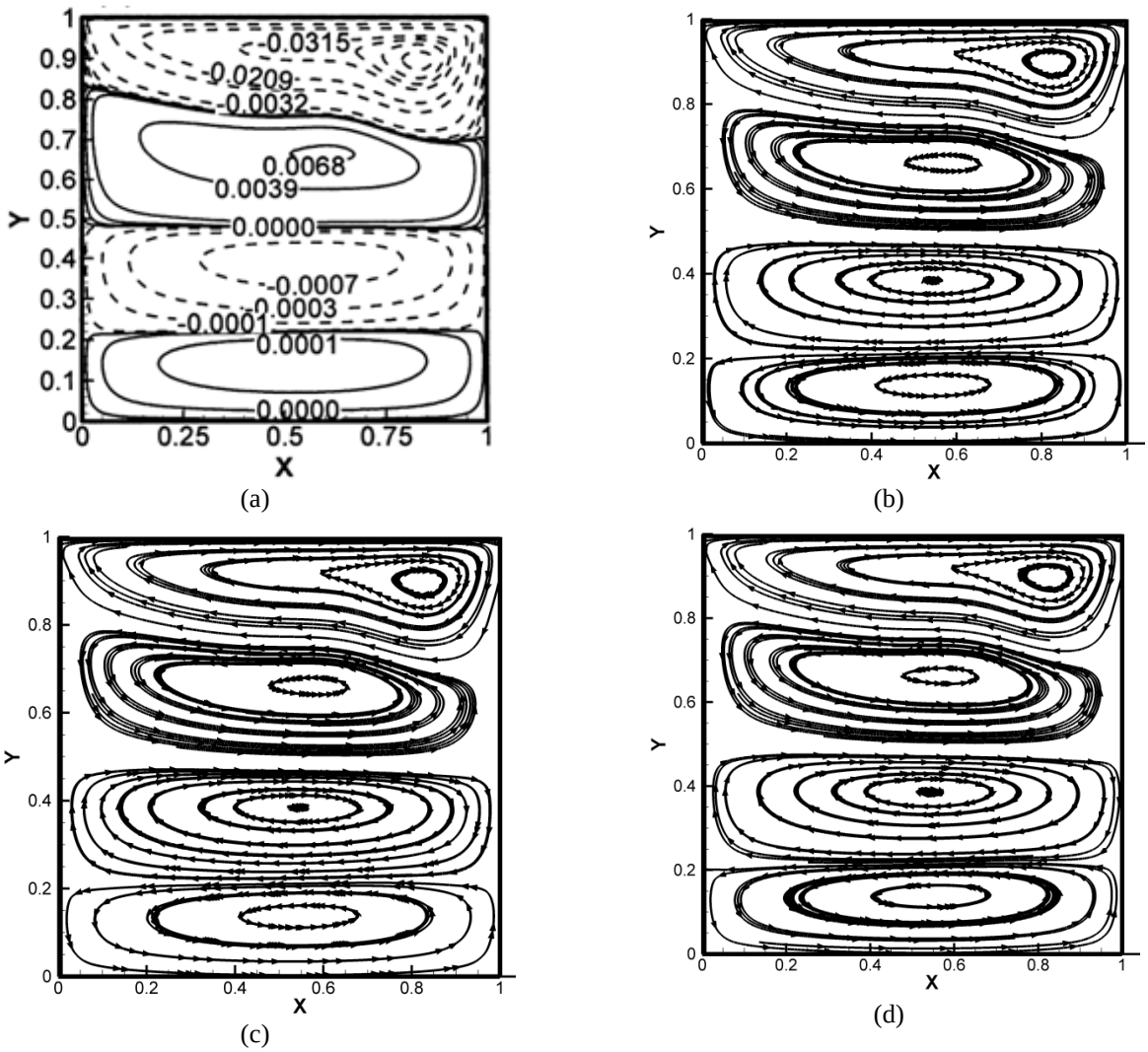

Fig. 8. Comparison of streamlines in different "β" with Cheng and Liu [14] results for Re=316, Pr=0.7 and Gr=1E6 (a) Cheng and Liu, (b) β=5, (c) β=25, (d) β=125.

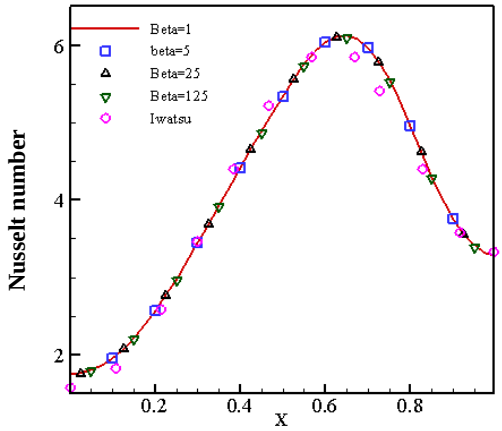

Fig. 9. Comparison of Nusselt number for up wall in different "β" with Iwatsu et al. [15] results for Re=400, Pr=0.7 and Gr= 100.

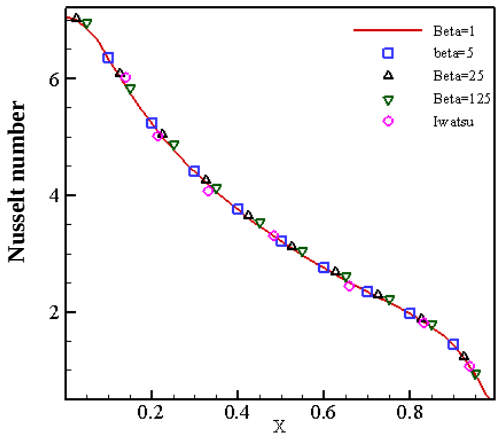

Fig. 10. Comparison of Nusselt number for down wall in different "β" with Iwatsu et al. [15] results for Re=400, Pr=0.7 and Gr=100.

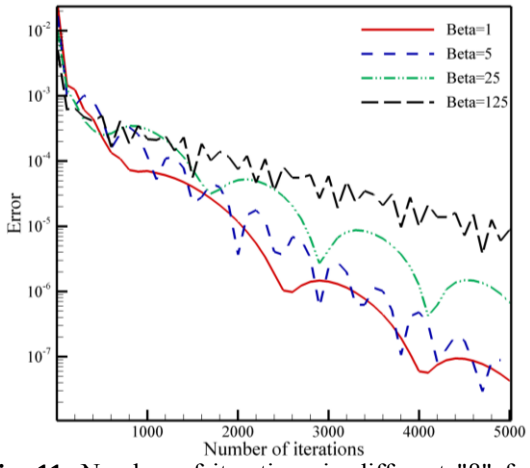

Fig. 11. Number of iterations in different "β" for Re=400, Pr=0.7, Gr=100.

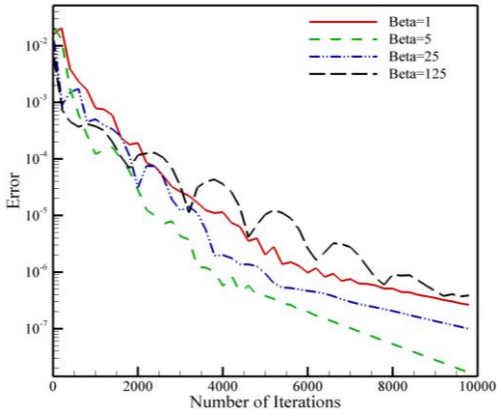

Fig. 12. Number of iterations in different "β" for Re=316, Pr=0.7, Gr=1E6.

Forced and mixed convection in cavity flow is simulated in different Grashof, Reynolds, and Prandtl numbers and in each simulation convergence history is obtained in the different artificial parameter. Convergence history that is obtained by different "β" is shown and compared in Figs. 11 and 12. Convergence history is influenced by "β". It seems the best "β" is between 1 and 5.

5. Conclusions

A new scheme for simulation of three-dimensional incompressible flows with heat transfer is presented. The convective fluxes are modeled using virtual characteristics. The new scheme benefits multidimensional characteristics, which are derived for the first time for thermo-flow equations with artificial compressibility. Since the new scheme applies characteristic compatibility equations, it presents stable solutions without any artificial dissipation even at higher Reynolds numbers. The cross-section of characteristic surfaces with the physical plane are obtained by the numerical solution. It is not a circle or oval, but as $\sqrt{\beta}$ tends to larger values, the cross-section could become a circle. The newly derived characteristic equations can be used for flux treatment in the finite volume method or data reconstruction in the finite difference method. The value of "β" does not change the results and their accuracy but it changes convergence history.

References

[1] D. Drikakis, P. A. Govatsos, and D. E. Papantonis, "A characteristic-based method for incompressible flows", *International journal for numerical methods in fluids*, Vol. 19, No. 8, p. 667-685, (1994).

[2] S. E. Razavi, and T. Adibi, "A novel multidimensional characteristic modeling of incompressible convective heat transfer", *Journal of Applied Fluid Mechanics*, Vol. 9, No. 4, (2016)

[3] T. Adibi, and S. E. Razavi, "A new-characteristic approach for incompressible thermo-flow in Cartesian and noncartesian grids", *International journal for numerical methods in fluids*, Vol. 79, No. 8, pp. 371-393, (2015).

[4] S. E. Razavi, and M. Hanifi, "A multi-dimensional virtual characteristic scheme for laminar and turbulent incompressible flows", *Journal of Applied Fluid Mechanics*, Vol. 9, No. 4, pp. 1579-1590, (2016).

[5] K. Zamzamian, and S. E. Razavi, "Multidimensional upwinding for incompressible flows based on characteristics", *Journal of Computational Physics*, Vol. 227, No. 19, pp. 8699-8713, (2008).

[6] R. Fathollahi, and K. Zamzamian, "An improvement for multidimensional characteristic-based scheme by using different selected waves", *International Journal for Numerical Methods in Fluids*, Vol. 76, No. 10, pp. 722-736, (2014).

[7] I. Abdollahi, K. Zamzamian, and R. Fathollahi, "High-accuracy upwind method using improved characteristics speeds for incompressible flows"," *International Journal for Numerical Methods in Fluids*, Vol. 80, No. 8, pp. 476-489, (2016).

[8] J. B. Franklin, and J. M. Harris, A high-order fast marching scheme for the linearized eikonal equation", *Journal of Computational Acoustics*, Vol. 9, No. 3, pp. 1095-1109, (2001).

[9] Van der Velden, W. C. P., J. T. Akhnoukh, and A. H. van Zuijlen, "Low-Order Finite-Volume Based Riemann Solver for Application to Aeroacoustic Problems", *Journal of Computational Acoustics*, Vol. 25, No. 3, pp. 175-185, (2017).

[10] R. Kaviani, and M. Nikkhah-Bahrami, "Improved Navier–Stokes Boundary Conditions Based on Generalized Characteristics", *Journal of Computational Acoustics*, Vol. 23, No. 2, pp. 155-161, (2014).

[11] A. Munir, M. Rizwan, and A. Shah, "Simulation of incompressible flow in two sided lid driven cavity using upwind compact scheme", *CFD LETTERS*, Vol. 5, No. 3, pp. 57-66, (2013).

[12] T. Adibi, R. A. Kangarluei, and V. Farhangmehr, "Numerical Study of Natural Convection Flow I nside Squared and Trapezoidal Cavities in Various Conditions", *International Journal of Science, Engineering and Technology Research*, Vol. 6, No. 5, pp. 2278-7798 (2017).

[13] C. Moyne, and H. P. A. Souto, "Multi-Scale approach for conduction heat transfer: one and two-equation models", *Computational and Applied Mathematics*, Vol. 33, No. 2, pp. 433-449, (2014).

[14] T. S. Cheng, and W.H. Liu, "Effect of temperature gradient orientation on the characteristics of mixed convection flow in a lid-driven square cavity", *Computers & Fluids*, Vol. 39, No. 6, pp. 965-978, (2010).

[15] R. Iwatsu, J. M. Hyun, and K. Kuwahara, "Mixed convection in a driven cavity with a stable vertical temperature gradient", *International Journal of Heat and Mass Transfer*, Vol. 36, No. 6, pp. 1601-1608, (1993).

How to cite this paper:

A. Tohid Adibi, "Three-dimensional characteristic approach for incompressible thermo-flows and influence of artificial compressibility parameter" *Journal of Computational and Applied Research in Mechanical Engineering*, Vol. 8, No. 2, pp. 223-234 (2019).

DOI: 10.22061/jcarme.2018.2032.1178

URL: http://jcarme.sru.ac.ir/?_action=showPDF&article=822